Lipopolysaccharide-Induced Apoptosis of Astrocytes: Therapeutic Intervention by Minocycline

Arpita Sharma, Nisha Patro & Ishan K. Patro

Cellular and Molecular Neurobiology

ISSN 0272-4340
Volume 36
Number 4

Cell Mol Neurobiol (2016) 36:577-592
DOI 10.1007/s10571-015-0238-y

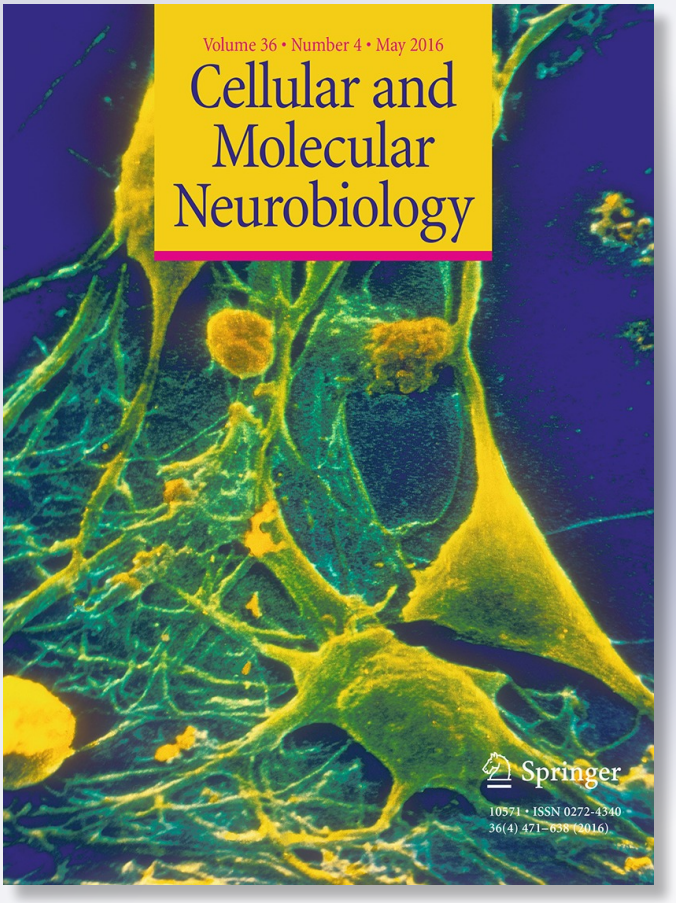

Springer

Cell Mol Neurobiol (2016) 36:577–592
DOI 10.1007/s10571-015-0238-y

ORIGINAL RESEARCH

Lipopolysaccharide-Induced Apoptosis of Astrocytes: Therapeutic Intervention by Minocycline

Arpita Sharma[1] · Nisha Patro[1] · Ishan K. Patro[1]

Received: 27 February 2015 / Accepted: 6 July 2015 / Published online: 19 July 2015

Abstract Astrocytes are most abundant glial cell type in the brain and play a main defensive role in central nervous system against glutamate-induced toxicity by virtue of numerous transporters residing in their membranes and an astrocyte-specific enzyme glutamine synthetase (GS). In view of that, a dysregulation in the astrocytic activity following an insult may result in glutamate-mediated toxicity accompanied with astrocyte and microglial activation. The present study suggests that the lipopolysaccharide (LPS)-induced inflammation results in significant astrocytic apoptosis compared to other cell types in hippocampus and minocycline could not efficiently restrict the glutamate-mediated toxicity and apoptosis of astrocytes. Upon LPS exposure 76 % astrocytes undergo degeneration followed by 44 % oligodendrocytes, 26 % neurons and 10 % microglia. The pronounced astrocytic apoptosis resulted from the LPS-induced glutamate excitotoxicity leading to their hyperactivation as evident from their hypertrophied morphology, glutamate transporter 1 upregulation and downregulation of GS. Therapeutic minocycline treatment to LPS-infused rats efficiently restricted the inflammatory response and degeneration of other cell types but could not significantly combat with the apoptosis of astrocytes. Our study demonstrates a novel finding on cellular degeneration in the hippocampus revealing more of astrocytic death and suggests a more careful consideration on the protective efficacy of minocycline.

✉ Ishan K. Patro
ishanpatro@gmail.com

[1] School of Studies in Neuroscience, Jiwaji University, Gwalior 474011, India

Keywords Astrocytes · Lipopolysaccharide (LPS) · Glutamine synthetase · Glutamate transporter-1 · Minocycline

Introduction

Astrocytes outnumber neurons by over fivefold and shape the microarchitecture of brain by forming the backbone of grey matter. They provide metabolic and trophic support to neurons, control extracellular ionic and neurotransmitter homoeostasis and protect neurons from oxidative stress and excitotoxicity (Zhao and Flavin 2000; Haydon and Carmignoto 2006; Verkhratsky and Butt 2007). Moreover, neuron astrocyte interaction associated release of neurotrophins, growth factors and neurosteroids by astrocytes are essential for the development and survival of neurons (Blanc et al. 1998; Kirchhoff et al. 2001; Garcia-Segura and McCarthy 2004). With much functional significance for neurons, any alteration in astrocytic pathway consequent to pathological stimuli may result in neuronal dysfunction.

Apart from these functions astrocytes by means of GLT transporters and astrocyte-specific enzyme glutamine synthetase (GS) also play central defensive role in clearing excessive toxic glutamate to non-toxic glutamine (Choi et al. 1987; Danbolt 2001; Shaked et al. 2002; Maragakis and Rothstein 2004), thereby preventing glutamate-induced neurotoxicity. Among various subtypes 90 % of glutamate uptake is carried by glutamate transporter 1 (GLT-1) subtype (Tanaka et al. 1997). Thus any stress to astrocytes can impair this function and may cause glutamate-mediated excitotoxicity. It has been reported that glutamate-mediated toxicity is initiated with the activation of both astrocytes and microglia (Kreutzberg 1996; Schousboe et al.

1997). Activated microglial cells release an array of proinflammatory cytokines and free radicals which regulate the expression of glutamate receptors (GluRs) and transporters on activated astrocytes modulating glutamatergic transmission and resulting in excitotoxic cellular damage (Tilleux et al. 2007; Tilleux and Hermans 2008). A sustained inflammatory response leading to increased level of cytokines also causes neuropathological conditions with impaired astrocytic function (Oliver et al. 1990; Huang and O'Banion 1998). Such impairment in astrocytic functions following glutamate excitotoxicity or an inflammatory response causes their degeneration and in turn alter the functions of nearby neurons and other astrocytes contributing to the pathogenesis of many acute and chronic neurological disorders (Suk et al. 2001; Chen and Swanson 2003; Takuma et al. 2004; Endale et al. 2010; Kim et al. 2010a, b). However, it is difficult to establish any direct contribution to glial or neuronal damage in vivo (Felts et al. 2005).

Lipopolysaccharide (LPS), a bacterial endotoxin is widely used to mimic systemic inflammatory conditions with activation of glial cells (microglia and astrocytes) in brain to synthesize and secrete a variety of neuroactive and neurotoxic molecules, interleukins and free radicals (Henry et al. 2008; Ghosh et al. 2014). Activated astrocytes proliferate and produce a variety of inflammatory mediators such as nitric oxide (NO), TNF-α, etc. that contribute to the pathogenesis of various neurodegenerative diseases (Sofroniew and Vinters 2010; Claycomb et al. 2013). Although there are reports indicating NO-mediated apoptosis of astrocytes in rat primary astrocyte culture exposed to a combination of LPS and inflammatory cytokines but not by either alone (Suk et al. 2001; Caruso et al. 2007; Quintas et al. 2014). In vivo studies stating intracerebroventricular (into lateral ventricle) LPS-induced astrocytic response in the hippocampus are scanty.

Minocycline, a semisynthetic tetracycline derivative has been proved to be neuroprotective by inhibition of microglial activation, apoptosis and suppression of reactive oxygen species production in various experimental models of neurological disorders (Plane et al. 2010). In addition, studies using experimental models of stroke also reported protective effects of minocycline on astrogliosis (Leonardo et al. 2008; Cai et al. 2010). Simultaneously other investigators indicated its ineffectiveness on astrogliosis and astrocytic apoptosis in stroke model indicating a complex action of this drug under same inflammatory conditions (Yrjanheikki et al. 1998; Matsukawa et al. 2009). Minocycline has also been reported to suppress LPS-induced neuroinflammation by suppressing microglial activation and associated cascade (Henry et al. 2008), and enhance oligodendroglial survival following LPS-induced inflammation (Guimaraes et al. 2010). However, the clear evidences as to how minocycline influences the LPS-induced astrocytic activation are still lacking.

This study hypothesizes for the first time that LPS-induced inflammation results in significant astrocytic apoptosis in the rat hippocampus via caspase-3-mediated pathway. Further, we confirm that the astrocytic apoptosis results from the LPS-induced glutamate excitotoxicity leading to their hyperactivation as evident from their hypertrophied morphology, GLT-1 upregulation and downregulation of GS. However, minocycline could not efficiently combat with this glutamate-mediated toxicity and apoptosis of astrocytes.

Materials and Methods

Animals

Forty-five adult Wistar rats (200–210 g) were taken from healthy stock of SOS in Neuroscience, Jiwaji University, Gwalior, in housed animal colony. The care and maintenance of all experimental animals was done as per CPCSEA guidelines. The rats were randomly divided into three groups as per the experimental design (Table 1). Animals were housed 3 per cage with dust-free rice husk as bedding material and maintained in standard conditions viz., 12 h light:dark cycle and controlled temperature of 23 ± 2 °C. The animals were fed with standard rat pellet diet and water ad libitum. All the experiments were pre-approved by the Institutional Animal Ethics Committee and the efforts were made to minimize the animal suffering during the experimental procedures.

Induction of Bacterial Infection by Intracerebroventricular Infusion of LPS

To create an in vivo LPS bacterial infection model, a single intracerebroventricular injection of LPS was given to each rat of 200–210 g body weight. The animals were deeply anaesthetized with a mixture of ketamine and xylazine and 2 μg of LPS (LPS, Escherichia coli, serotype 0111: B4, Sigma), dissolved in 2 μl of sterilized PBS was injected unilaterally into the right lateral ventricle at the coordinates: 0.8 mm posterior, 1.8 mm right to midline and 3.0 mm ventral to bregma (Paxinos and Watson 1982) using a stepper motorized injector mounted on a stereotaxic apparatus (Stoelting, USA) at a rate of 0.2 μl/min. The animals were revived from anaesthesia and maintained in sterilized cages. Half of the LPS-infused animals were marked as group-II, while other half were therapeutically treated with minocycline and constituted group-III. An equal volume of PBS was infused similarly in a group of animals which served as vehicle control group-I.

Table 1 Experimental design

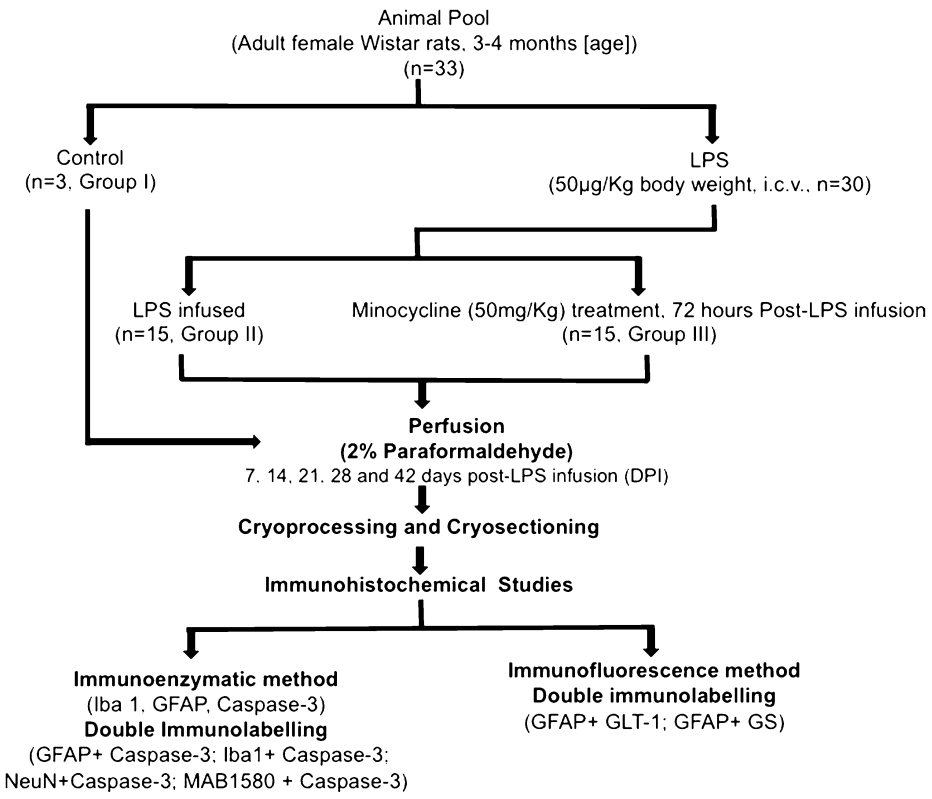

Therapeutic Treatment by Minocycline

72 h post-LPS infusion half of the LPS-infused animals were treated with minocycline hydrochloride (Sigma) twice daily for seven consecutive days at a dose of 50 mg/kg body weight. Fresh solution of minocycline was prepared each day by dissolving in sterile endotoxin-free isotonic 0.9 % saline and administered intraperitoneally (i.p.). This group served as group-III.

Perfusion and Tissue Processing

In order to study the time course of the inflammatory reaction, apoptosis and the protective efficacy of the drug, rats were sacrificed at different time points, i.e. 7, 14, 21, 28 and 42 day post-LPS infusion (DPI) from all the three groups. The rats were anaesthetized with diethyl ether and perfused transcardially first with cold phosphate-buffered saline followed by 2 % paraformaldehyde prepared in phosphate buffer (0.01 M; pH 7.4). Fore brain tissues from the occipitotemporal region were dissected out and post fixed in the same fixative at 4 °C, overnight. The tissues were then cryoprotected with sucrose gradients, i.e. 10, 20 and 30 % sucrose in phosphate buffer. Coronal sections of forebrain from occipitotemporal region through hippocampus were cut at a thickness of 15 µm using a Leica Cryotome CM1900 and collected on chromalum gelatin-coated slides. The slides were further stored at −20 °C for immunohistochemical analysis.

Immunohistochemical Studies

Immunohistochemical studies through immunoenzymatic method were performed to assess the neuroinflammatory response following LPS infusion at various time points. Randomly selected cryocut sections from each parameter were dried at room temperature (RT) and permeabilised with 1 % triton X 100 (Sigma) in PBS for 30 min. The tissues were treated with 1 % hydrogen peroxide (Qualigens) in PBS for endogenous peroxidase blocking followed by washing with PBS. Non-specific proteins were blocked by incubating sections in 1 % normal goat serum (Sigma) to minimize background staining. The sections were then incubated with the primary antibodies [anti-Iba1(rabbit polyclonal, 1:400; Wako, Japan) for microglial activation, anti-OX-6 (mouse monoclonal, 1:100, Serotec) for MHC II

expressing antigen-presenting cells, anti-GFAP (rabbit polyclonal, 1:2000; Dako, Denmark) for astrocytic activity and anti-active Caspase-3 (rabbit polyclonal, 1:4000; R&D Systems) for localizing apoptotic cells] diluted in 1 % Bovine Serum albumin (BSA, Himedia) in PBS at 4 °C overnight. Next day the sections were brought to RT washed in PBS, incubated with anti-rabbit/anti-mouse biotin-labelled secondary antibody (Sigma) for 60 min at RT. After washing with PBS, the sections were incubated with streptavidin–biotin HRP complex (SABC, 1:200; Amersham) for 60 min. The antigens were visualized by incubating the sections in chromogen solution containing 0.025 % 3, 3′-diaminobenzidine tetrahydrochloride (DAB, Sigma) or with 0.025 % DAB enhanced with 2.5 % nickel sulphate hexahydrate ($NiSO_4$, Sigma) and 0.06 % H_2O_2 for 20 min. The reaction was terminated by washing the sections with water. The sections were then air dried, dehydrated, cleared in xylene, covered with DPX and coverslipped.

Double Immunolabelling by Immunoenzymatic Method

To determine the proportion of cell types undergoing Caspase-3-mediated apoptosis, a sequential staining protocol was used to avoid problems related to cross reactivity. The sections were incubated first with primary antibody, i.e. rabbit polyclonal anti-GFAP (1:10,000; Dako)/rabbit polyclonal anti-Iba1 (1:800; Wako)/mouse monoclonal anti-NeuN (1:100; Chemicon)/mouse monoclonal anti MAB 1580 (1:2000; Oligodendrocyte marker; Chemicon) prepared in 1 %BSA in PBS overnight at 4 °C. Next day the sections were buffer washed and incubated with the appropriate biotin-labelled secondary antibody (1:100; Sigma) followed by incubation in streptavidin–biotin HRP complex (SABC, 1:200; Amersham). The antigens were finally visualized with 0.025 % 3, 3′-diaminobenzidine tetrahydrochloride (DAB; Sigma) and 0.06 % hydrogen peroxide. For completely eluting the primary and secondary antibodies from first staining, the sections were rigorously washed and incubated with 1 % NGS for 2 h at RT to block the non-specific protein and then incubated with second primary antibody, i.e. rabbit polyclonal anti-active caspase-3 (1:4000; R&D) antibody at 4 °C, overnight. Third day, the sections were brought to RT, incubated with anti-rabbit biotin-labelled (1:100; Sigma) secondary antibody followed by washing with buffer and further incubation with streptavidin-biotin-HRP complex (1:200; Amersham). Sections were finally incubated with nickel-enhanced DAB (0.025 % DAB + 0.06 % H_2O_2 and 2.5 % $NiSO_4$ dissolve in 100 ml of buffer) for antigen visualization. Each of the above steps was followed by three 5-min rinses in PBS. The sections were finally washed with distilled water, air dried, dehydrated, cleared in xylene and coverslipped with DPX.

Immunohistochemistry for Glutamine Synthetase (GS) and Glutamate Transporter-1 (GLT-1)

The expression of GS and GLT-1 in astrocytes was examined through simultaneous staining double immunofluorescence method. Cryocut sections selected from various parameters were air dried at RT and permeabilised with 1 % triton X-100. Non-specific proteins were blocked using 5 % BSA in PBS for 1 h prior to incubation in cocktail of primary antibodies i.e. guinea pig polyclonal anti-GLT-1 (1:2000; Chemicon) + rabbit polyclonal anti-GFAP (1:2000; Dako) and mouse monoclonal anti-GS (1:2000; Chemicon) + rabbit polyclonal anti-GFAP (1:2000; Dako) at 4 °C for 48 h. After 48 h incubation the sections were washed and further incubated with an appropriate combination of fluorochrome-tagged secondary antibodies (Cy3-labelled goat anti-guinea pig IgG 1:500; Sigma + FITC conjugate anti-rabbit IgG or TRITC conjugate anti-mouse IgG + FITC conjugate anti-rabbit IgG) at a dilution of 1:500 for 1 h in dark. The sections after proper washing in PBS were finally mounted with Vector mounting medium i.e. hardset with DAPI and stored at 4 °C in dark.

Quantification and Image Analysis

All immunostained slides were visualized using Leica DM 6000 microscope and the images were captured with a Leica DFC420 RC digital camera attached to it using Leica application suite (LAS) software (Leica, Germany). Images from each parameter were taken from distinct areas of hippocampus i.e. Cornu Ammonis (CA1, CA2, CA3) and dentate gyrus (DG) with a total of eight different images, two per region. Immunoreactivity was quantified using interactive method of Leica QWin software (Leica, Germany). A total of 8 frames of hippocampal region per section were randomly selected. The area of each frame was defined by 21670.9 μm^2 in order to maintain uniformity for cell count for each representative image. The data obtained were then converted to number of immunostained cells per mm^2 and the mean was calculated. All images subjected to quantification studies were captured using identical exposure limit, gain, saturation, shading and filter to abolish inconsistency in background intensity or false-positive immunoreactivity across sections.

Statistical Analysis

In order to examine the level of significance the data recorded was analysed statistically using One Way

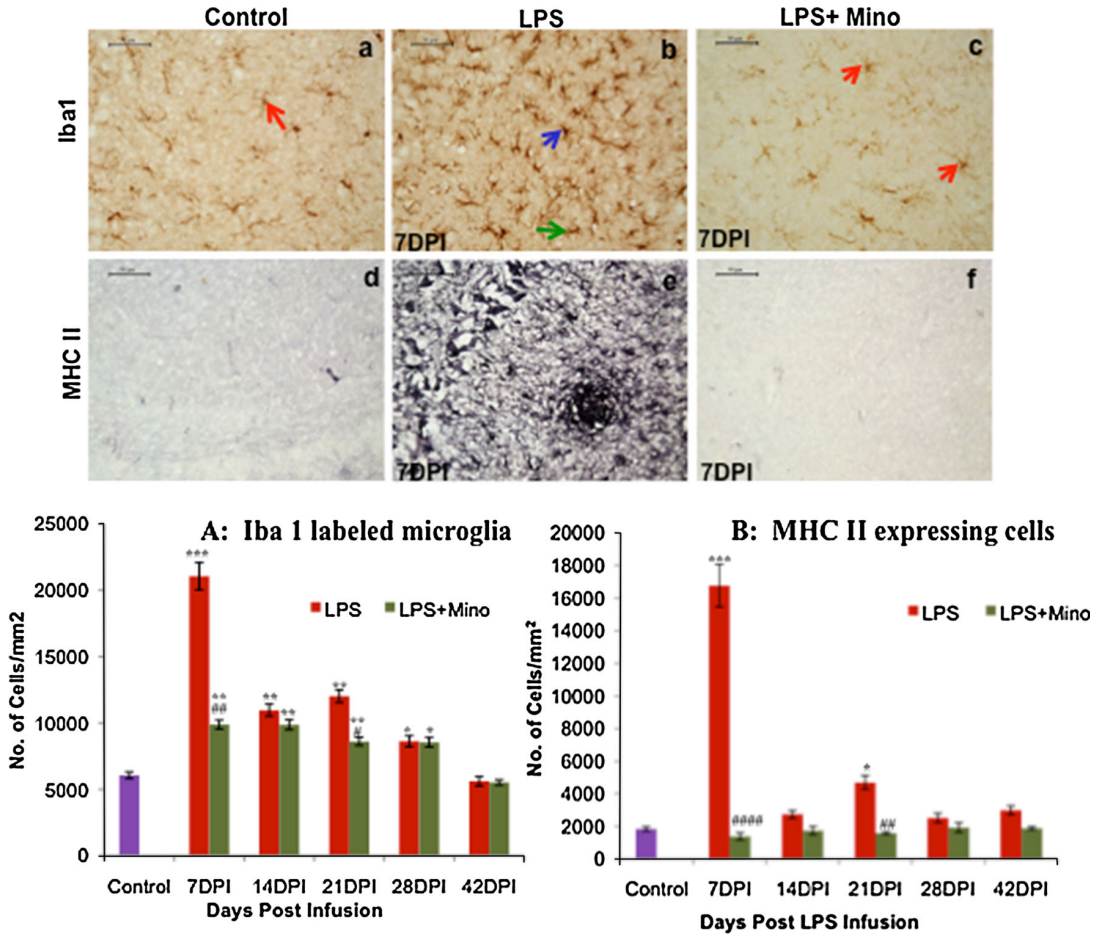

Fig. 1 Light microscopic images depicting LPS-induced microglial activation and MHC II expression in the CA3 subfield of rat hippocampus: Microglial activation indicated by activated phenotypes with shorter and thicker processes, larger cell soma and strong Iba 1 labelling (*blue arrows*) and some *full blown* phagocytic or amoeboid microglia (*green arrow*; **b**) as compared to resting or ramified microglia with small cell soma and several thin and long processes in controls (*red arrows*; **a**), minocycline treatment effectively attenuated the LPS-induced microglial activation (**c**); Enhanced MHC II expression as revelled by intense OX-6 labelling throughout the region (**e**) in contrast to almost nil in controls (**d**), minocycline treatment completely restricted MHC II expression (**f**). *Scale bar* 50 µm. Morphometric studies revealed a significant increase in both Iba-1-labelled microglia (**A**) and MHC II expressing cells (**B**) after LPS infusion. The cell count was significantly reduced after minocycline treatment. Values are expressed as mean ± SEM; $^{*}P \leq 0.05$, $^{**}P \leq 0.01$, $^{***}P \leq 0.001$ with respect to controls; $^{\#}P \leq 0.05$, $^{\#\#}P \leq 0.01$, $^{\#\#\#\#}P \leq 0.0001$ with respect to LPS group (Color figure online)

Analysis of Variance (ANOVA) followed by Tukey's post hoc test using Sigma Stat 3.5 software. Statistical significance was preset at $P \leq 0.05$.

Results

Protective Approach of Minocycline on Innate Immune Response Following LPS Infusion

LPS infusion resulted in profound microglial activation as depicted by the activated and amoeboid morphology in contrast to the normal ramified microglia in vehicle controls (Fig. 1a, b). Some of the microglia got transformed into the antigen-presenting cells as evident by the MHC II expression on their surface following OX-6 labelling (Fig. 1e). However, no MHC II expressing cells were noted in the respective controls (Fig. 1d). The cell count for both the total number of microglia (Fig. 1A) and the MHC II expressing cells (Fig. 1B) increased significantly in the hippocampus of LPS group animals. Astrocytic activation was also observed both in terms of hyperplasia and hypertrophy. The reactive astrocytes appeared hypertrophic with numerous longer and thickened processes and enhanced GFAP expression (Fig. 2b) in contrast to the normal morphology in the vehicle controls (Fig. 2a). A sizeable number of GFAP-labelled dystrophic astrocytes were also recorded indicating the degenerative changes. The hyperplasia was evident from a significant

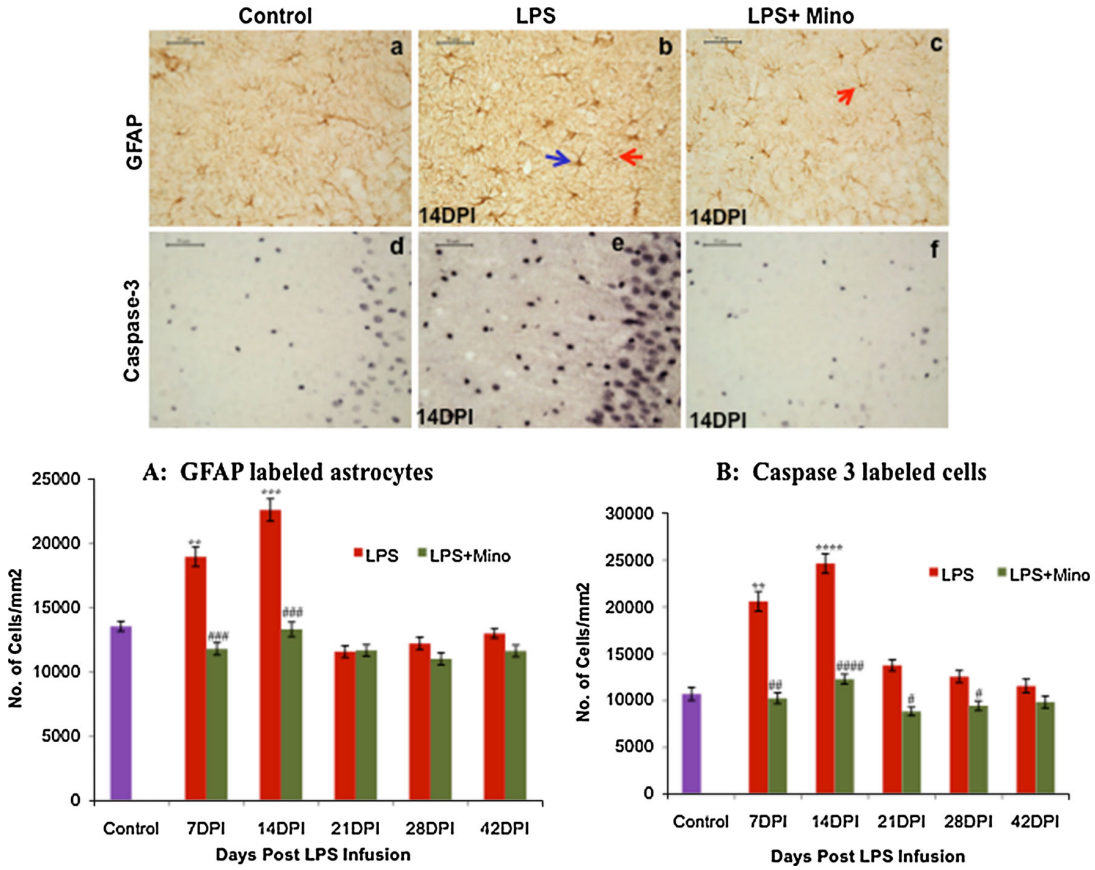

Fig. 2 GFAP immunostaining revealed astrocytic activation with hypertrophied (*blue arrow*) and dystrophic astrocytes (*red arrow*) after LPS treatment (**b**) in comparison with normal star-shaped astrocytes in controls (**a**) and reduced activation after minocycline treatment (**c**); active caspase-3 immunostaining revealed a large number of strongly caspase-3-labelled cells in LPS-infused sections (**e**) in contrast to controls (**d**) and drastically reduced after minocycline treatment (**f**). *Scale bar* 50 µm. Morphometric studies revealed astrocytic (**A**) as evaluated by the counting of GFAP-labelled cells and increased apoptosis as evident from the number of active Caspase-3-labelled cells (**B**). The cell count of these cell types was reduced after minocycline treatment. Values are expressed as mean ± SEM; $^{**}P \leq 0.01$, $^{***}P \leq 0.001$, $^{****}P \leq 0.0001$ with respect to controls; $^{\#}P \leq 0.05$, $^{\#\#}P \leq 0.01$, $^{\#\#\#}P \leq 0.001$, $^{\#\#\#\#}P \leq 0.0001$ with respect to LPS group (Color figure online)

increase in cell count of astroglia throughout the hippocampus (Fig. 2A). Such changes were most prominent in CA3 region followed by DG and CA1. Therapeutic minocycline treatment to LPS-infused animals could effectively restrict the activation of both microglia (Fig. 1c, f) and astrocytes (Fig. 2c, f) as well as reduced the population of microglia (Figs. 1A, B) and astrocytes (Fig. 2A) thereby, suggesting its protective ability to ameliorate inflammatory response in brain.

Minocycline Restricts LPS-Induced Caspase-3 Mediated Apoptosis

LPS infusion resulted in a significant active caspase-3 immunolabelling that revealed a strong positivity in a large number of cells throughout the hippocampus (Fig. 2e). However, a few very mildly labelled cells were also seen in respective vehicle control group preparations (Fig. 2d). Cell count analysis of active caspase-3-labelled cells indicated a significant and time-dependent linear increase following LPS infusion with a peak number of apoptotic cells at 14DPI (Fig. 2B) indicating an activation-induced cell death. Minocycline administration effectively limited the apoptosis of cells by restricting the LPS-induced glial activation (Fig. 2f, B).

Keeping in view that LPS infusion resulted in an appreciable increase in the number of caspase-3-positive cells, we further focussed to determine the proportion of different cell types undergoing apoptosis using cocktail of antibodies in both the infected and therapeutic groups.

Therapeutic Minocycline Administration Partially Effective on Activation-Induced Apoptosis of Astrocytes

In the first set of experiment on colabelling study, colocalization of GFAP and active caspase-3 in hypertrophied

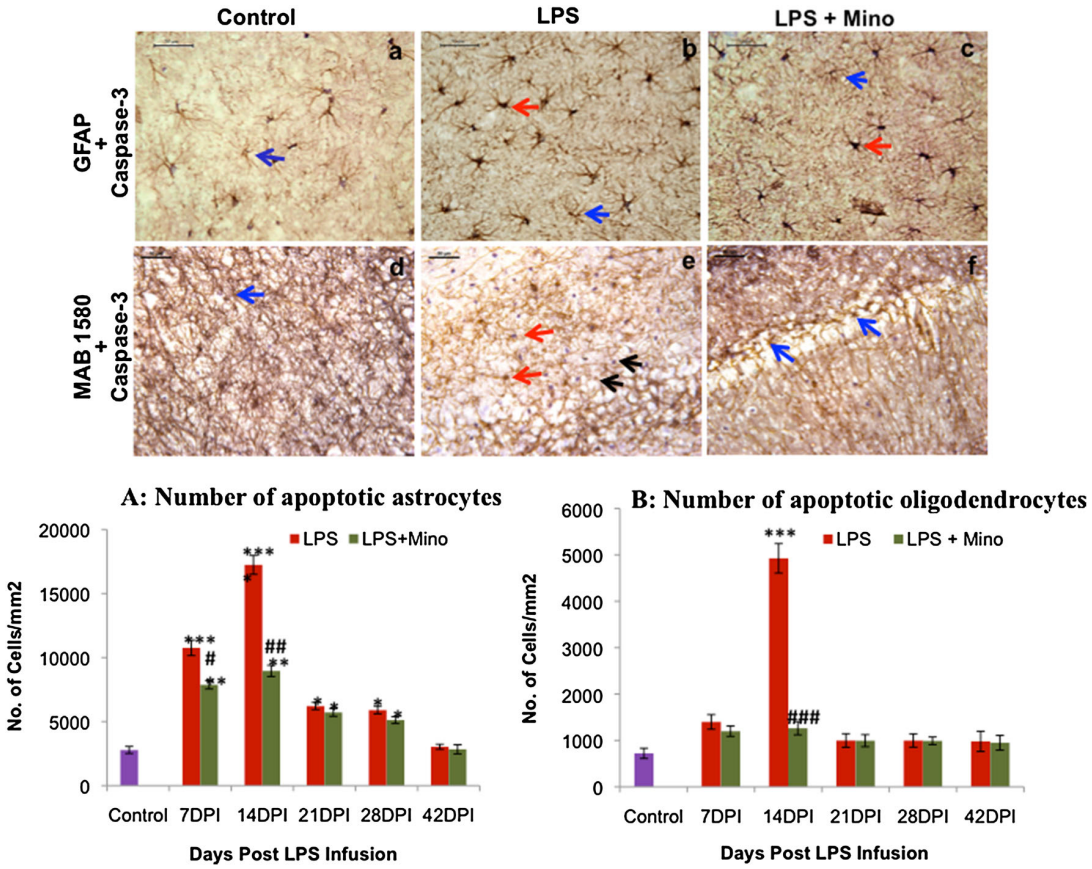

Fig. 3 Astrocytic and oligodendroglial apoptosis shown by double immunolabelling for active Caspase-3 and their specific markers, i.e. GFAP (**a**–**c**) and oligodendrocytes (**d**–**f**), respectively in the CA3 region of hippocampus. *Red arrows* indicate colabelled cells, *blue arrows* show non-colabelled astrocytes or oligodendroglia, while *black arrows* present non-colabelled caspase-3-positive cells. *Scale bar* 50 μm. Histograms showing the number of apoptotic astrocytes (**A**) as the mean total astrocytes colabelled with caspase-3 and the number of apoptotic oligodendroglia (**B**) as the mean total oligodendrocytes colabelled with caspase-3. Values are expressed as mean ± SEM.$^{*}P \leq 0.05$, $^{**}P \leq 0.01$, $^{***}P \leq 0.001$, $^{****}P \leq 0.0001$ with respect to controls; $^{\#}P \leq 0.05$, $^{\#\#}P \leq 0.01$, $^{\#\#\#}P \leq 0.001$, with respect to LPS group (Color figure online)

astrocytes indicated the apoptosis of activated astrocytes. The results showed a significant increase (64 %) in the number of colabelled cells throughout hippocampus at 7DPI with reference to the controls (Fig. 3A; $F_{(2,137)} = 13.616$; $P \leq 0.0001$). By 14DPI, a further increase in the number of apoptotic astrocytes (76 %) was recorded which was highly significant with respect to controls (Figs. 3a, 5a; $F_{(2,137)} = 15.21$; $P \leq 0.0001$) where only 20 % of the astrocytes were colabelled with active caspase-3 (Figs. 3A, 6). In the hippocampus, these colabelled cells were more pronounced in the CA3 (Figs. 3b, 5b, 10a, b) and DG (Fig. 10g, h) regions, while only a very few cells were recorded in the other hippocampal subfields, i.e. CA1 and CA2. From 21DPI onwards these colabelled astrocytes decreased linearly up to 42DPI. At 42DPI the difference in colabelled cell count was not significant with respect to the vehicle controls indicating a restoration of normal conditions (Figs. 3A, 4).

Minocycline treatment to the LPS-infused rats significantly attenuated the LPS-induced caspase-3-mediated apoptosis (Fig. 2B), as well as astrocytic apoptosis (Fig. 3A). This reduction in the number of apoptotic astrocytes was quite evident and highly significant at 14DPI ($F_{(2,137)} = 4.290$; $P \leq 0.05$) when a peak number of apoptotic astrocytes were recorded following LPS infusion. Although there was an overall decrease in the number of apoptotic astrocytes following minocycline treatment, the percent population of active caspase-3 colabelled astrocytes did not alter much. A 67 % of reactive astrocytes still colabelled with caspase-3 at 14DPI (Figs. 3A, c, 5c) in comparison with the 76 % colabelled astrocytes in LPS alone (Fig. 6), indicating thereby that although minocycline acts as

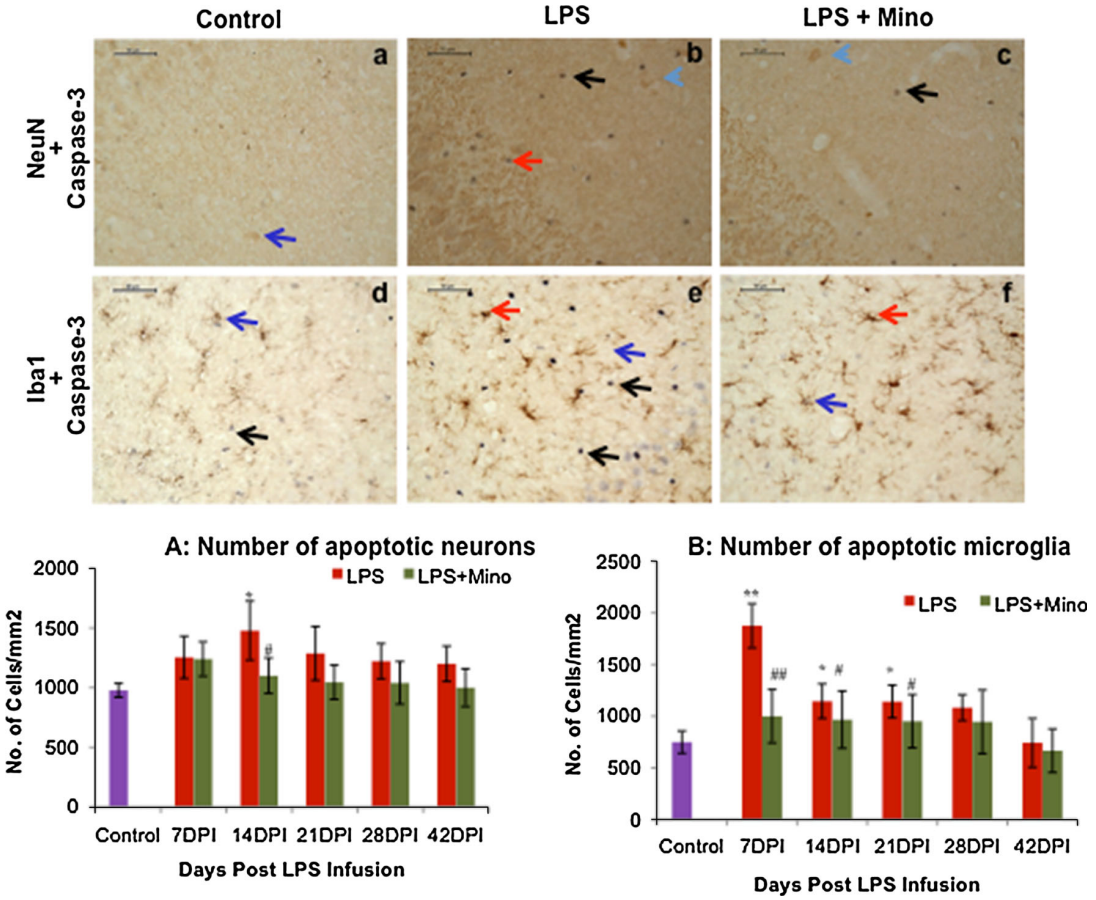

Fig. 4 A very few neurons and microglia undergo apoptosis as depicted by colabelling studies for caspase-3 with NeuN for neurons (**a**–**c**) and Iba1 for microglia (**d**–**f**) in the CA3 region of hippocampus at 14DPI. *Red arrows* indicate colabelled cells, *blue arrows* non-colabelled cells while *black arrows* non-colabelled caspase-3-positive cells. *Scale bar* 50 μm. Graphs (**A**) represent the mean total neurons colabelled with caspase-3 and the mean total microglia (**B**) colabelled with caspase-3 in hippocampus region of three groups. Values are expressed as mean ± SEM $^{*}P \leq 0.05$, $^{**}P \leq 0.01$, $^{***}P \leq 0.001$, $^{****}P \leq 0.0001$ with respect to controls; $^{\#}P \leq 0.05$, $^{\#\#}P \leq 0.01$, $^{\#\#\#}P \leq 0.001$, with respect to LPS group (Color figure online)

an apoptotic inhibitor, it does not influence the astrocytic apoptosis effectively.

Minocycline Administration Improved Glutamine Synthetase (GS) Expression in Hippocampal Astroglia

To further understand the mechanism of the astrocytic apoptosis following LPS infusion, the expression of markers for astrocytic activity like GLT-1 and GS was studied. GS, an astrocyte-specific enzyme converts glutamate to glutamine and thus participates in glutamate clearance. Since our results indicate the LPS-induced hypertrophy and apoptosis of astrocytes in the areas rich in glutamatergic synapses, the expression of GS in these astrocytes was examined.

As shown in Fig. 7a–d, most of the resting astrocytes (93 %) in controls colabelled clearly for GFAP and GS. In contrast, in the hippocampus of the rats 7-day post-LPS infusion, there was a significant downregulation in GS expression (Fig. 9; $F_{(2,137)} = 6.223$; $P \leq 0.01$] along with a decrease in number of astrocytes expressing GS (49 %) as compared with the vehicle controls. A further decrease in GS expression was noticed by 14DPI (Fig. 8; $F_{(2,137)} = 8.015$; $P \leq 0.001$) where only 30 % of the astrocytes were expressing GS. Most of the GS-negative cells were either hypertrophied or dystrophic, restricted mostly to the CA3 (Figs. 7e–h, 10d) and DG region (Fig. 10j) in their location as compared to normal GS expressing astrocytes of control group (Figs. 7a, 10c, i). However, at 21DPI and thereafter the GS expression was effectively resumed along with a decrease in the number of

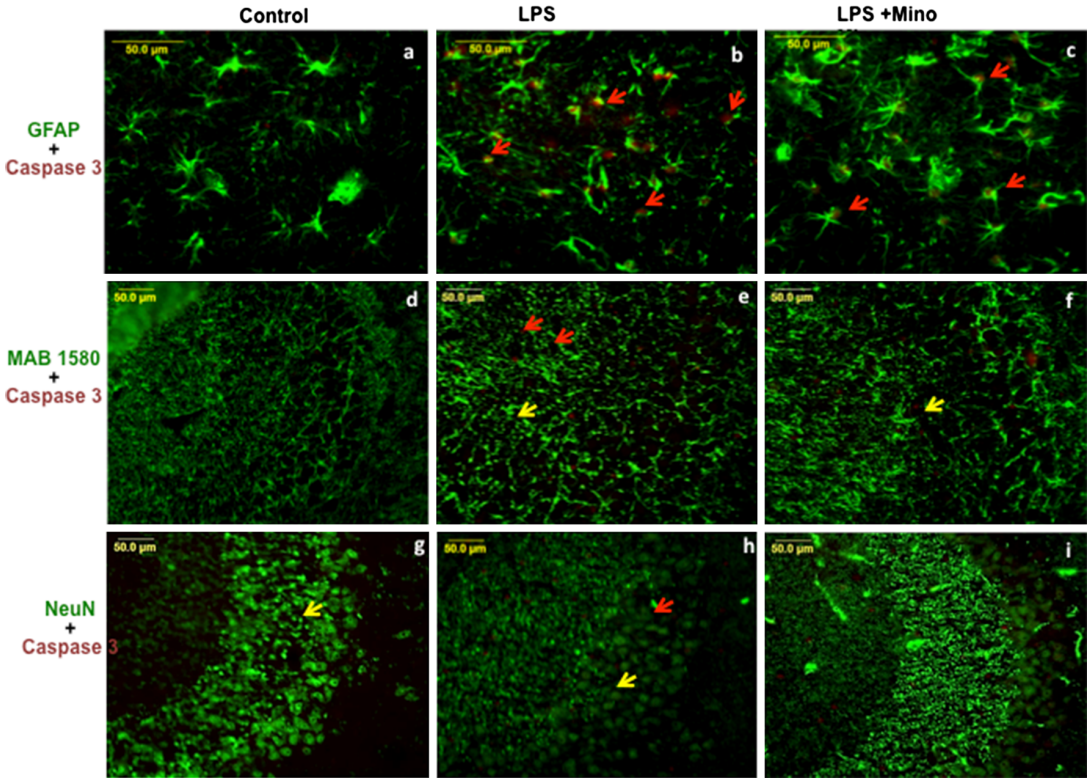

Fig. 5 Dual immunofluorescence images with GFAP + caspase-3 (**a**–**c**); MAB 1580 + caspase-3 (**d**–**f**); and NeuN + caspase-3 (**g**–**i**) in CA3 region of the hippocampus summarizing selective astrocytic apoptosis following LPS infusion. *Red arrows* indicate colabelled cells, *yellow arrows* non-colabelled cells. *Scale bar* 50 µm (Color figure online)

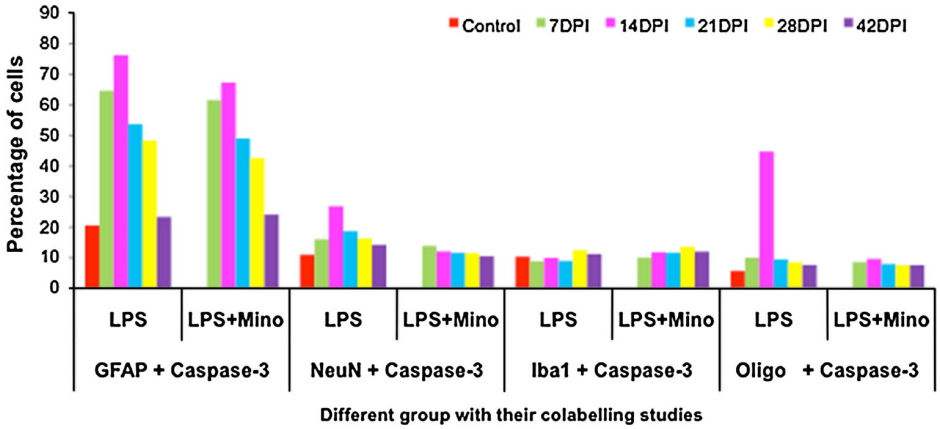

Fig. 6 Histogram showing the comparative view on the percentage of apoptotic cells from the total number of respective glial or neuronal cells at 14DPI. Astrocytic apoptosis predominates following LPS infusion followed by oligodendrocytes with negligible neuronal and microglial apoptosis. LPS + minocycline-treated rats also depicted more of astrocytic degeneration

hypertrophied astrocytes and was quite similar to controls by 42DPI.

This was evident from 7DPI when 84 % of astrocytes in the hippocampus were brightly labelled with GS showing normal morphology. By 14DPI, there was a further decrease in the number of GS colabelled astrocytes with only 70 % astrocytes coexpressing GFAP and GS. These GS-negative astrocytes were hypertrophied and were visible in the CA3 and DG regions. Following minocycline treatment although the intensity of GS labelling improved both at 7 and 14DPI (Fig. 9; $F_{(2,137)} = 4.823$, 4.462; $P \leq 0.01$, $P \leq 0.05$) from the respective LPS group but was yet significantly low at 14DPI as compared to the controls (Fig. 9; $F_{(2,137)} = 5.40$; $P \leq 0.05$]. From 21DPI onwards up to 42DPI, such dystrophic and hypertrophied astrocytes lacking GS activity were almost negligible with quite similar expression to vehicle controls in both the LPS and LPS + minocycline groups.

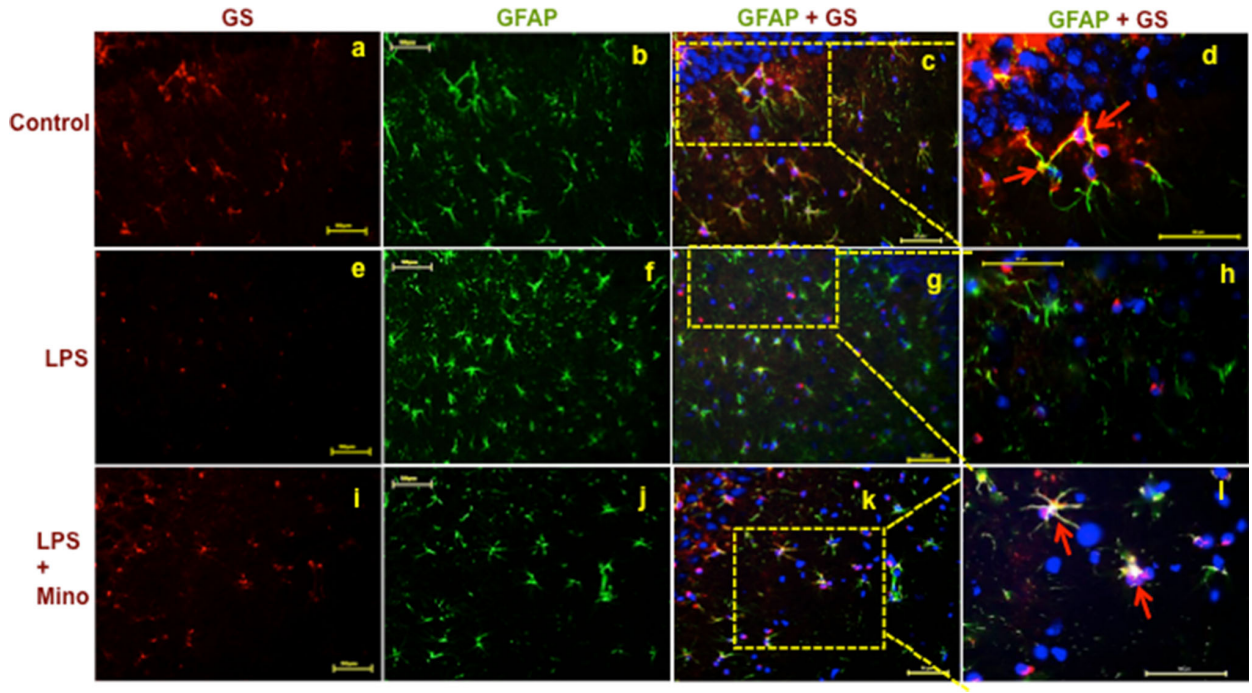

Fig. 7 Dual immunofluorescence staining with GFAP and GS in the CA3 region of the hippocampus. GS (*red*, **a**, **e**, **i**) and GFAP (*green*; **b**, **f**, **j**). Overlay images (**c**, **g**, **k**) indicate the expression of GS in GFAP + astrocytes (*red arrows*). GS expression is downregulated (**e**) in hypertrophied astrocytes (**f**) following LPS infusion which was restored after minocycline treatment (**i**, **j**). Images **d**, **h** and **i** are the higher magnification images of the *boxed* areas in images **c**, **g** and **k**, respectively. *Scale bar* 50 μm (Color figure online)

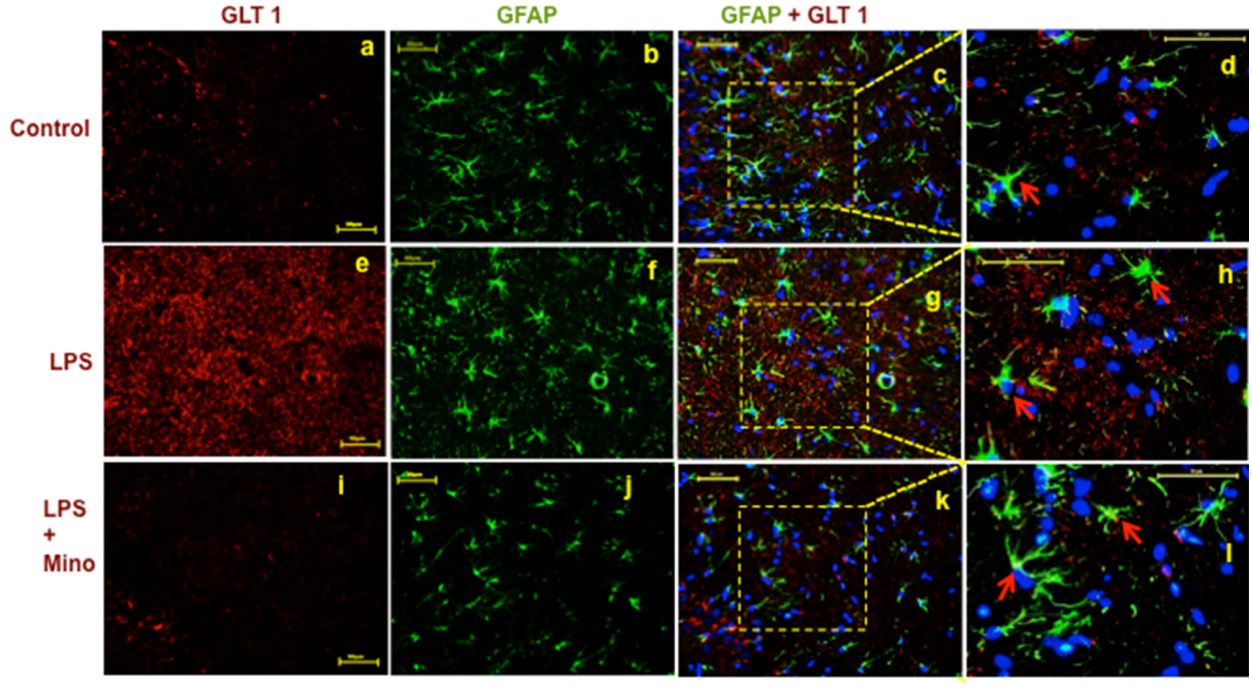

Fig. 8 Dual immunofluorescence staining with GFAP and GLT-1 in the CA3 region of the hippocampus. GLT-1 (*red*, **a**, **e**, **i**), GFAP (*green*; **b**, **f**, **j**) and merged images (**c**, **g**, **k**). GLT-1 expression was upregulated (**e**) in hypertrophied astrocytes (*red arrows*; **f**) following LPS infusion which was restored to near control (**a**) after minocycline treatment (**i**). Images **d**, **h** and **i** are the higher magnification images of the *boxed* areas in images **c**, **g** and **k**, respectively. *Scale bar* 50 μm (Color figure online)

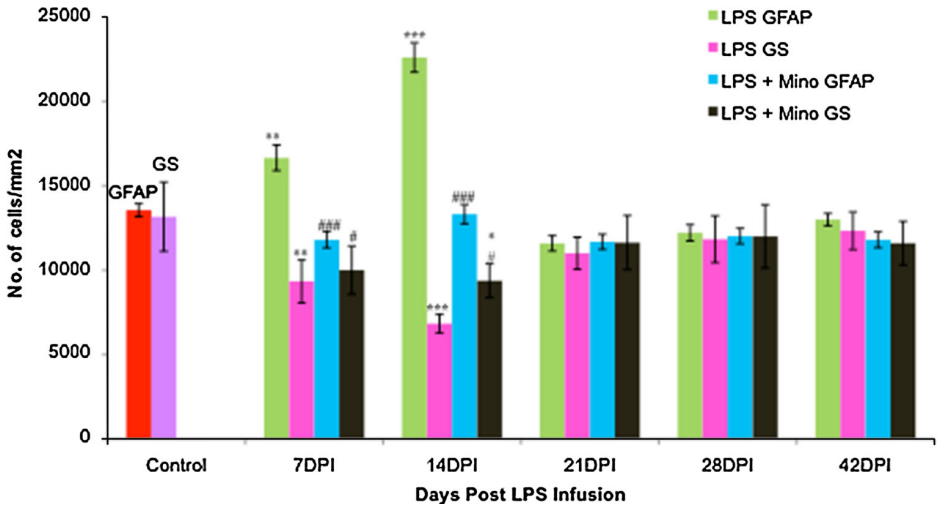

Fig. 9 Histogram showing the number of GFAP- and GS-labelled cells. Values are expressed as mean ± SEM.*$P \leq 0.05$, **$P \leq 0.01$, ***$P \leq 0.001$ with respect to controls; $^{\#}P \leq 0.05$ with respect to LPS group

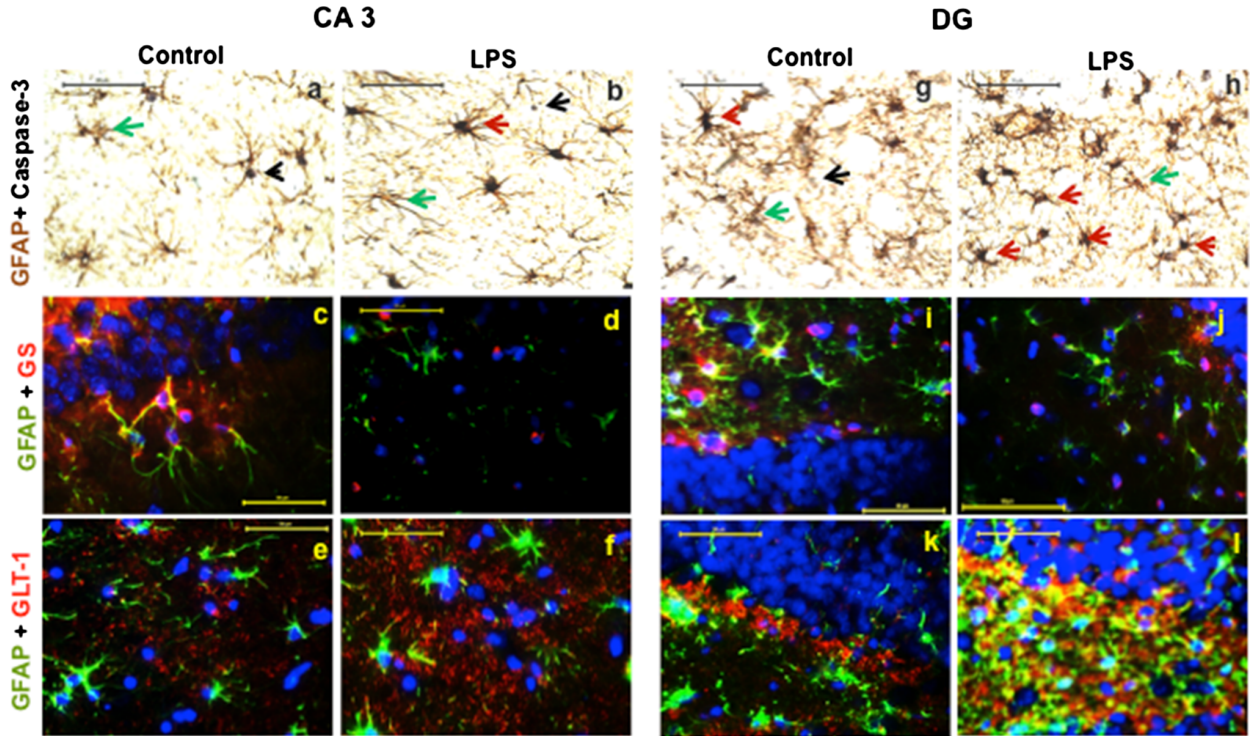

Fig. 10 Double immunostaining images summarizing the LPS-induced astrocytic apoptosis, GS downregulation and GLT-1 upregulation following LPS infusion in CA3 (**a**–**f**) and DG (**g**–**l**) regions of the hippocampus. *Red arrow* indicates colabelled astrocyte, *green arrow* shows non-colabelled astrocyte and *black arrow* indicates non-colabelled caspase-3-positive cell. *Scale bar* 50 µm (Color figure online)

Protective Approach of Minocycline by Limiting the Expression and Activity of GLT-1 in Hippocampal Astrocytes

One of the major functions of reactive astrocytes is to regulate extracellular levels of glutamate in areas of brain injury and thus potentially mitigating excitotoxic injury via efficient glutamate transport carried out by GLT-1 transporters. Keeping the LPS-induced reactive astrogliosis in view, the expression of GLT-1 transporters on astrocytes was evaluated. The results revealed considerable expression of GLT-1 transporters both on the membrane of the

cell body and processes of astrocytes in controls as revealed by colabelling with GFAP (Fig. 8a–d). Consistent with an increase in the number of reactive astrocytes at 7DPI an increase in GLT-1 transporter was also evident. By 14DPI a sharp increase in GLT-1 expression on reactive astrocytes in CA3 region (Figs. 8e, 10f) was noticed followed by DG (Fig. 10i) as compared to vehicle controls (Fig. 10e, k). Most of the hypertrophied astrocytes were heavily expressing GLT-1 transporters (Fig. 7e). Furthermore, this GLT-1 expression was also noticed in the spaces between pyramidal neurons, indicating the processes of astrocytes to be tightly surrounding them. From 21DPI onwards, a decline in GLT-1 expression was noticed throughout the hippocampal regions and appeared to be returning to normal conditions as no difference with vehicle controls was noticed by 42DPI post-LPS infusion.

Minocycline treatment to LPS-infused rats effectively downregulated the expression of GLT-1 in the hippocampus. The downregulation in GLT-1 expression on astrocytes both at 7 and 14DPI in minocycline-treated LPS-infused rats was sharply demarcated. However, at 14DPI, few hypertrophied astrocytes in CA3 region were still brightly labelled with GLT-1 (Figs. 8i–l). By 21DPI and thereafter these hypertrophied astrocytes as well as GLT-1 expression was less with no difference in GLT-1 expression on astrocytes at 42DPI with respect to vehicle controls.

Minocycline Effectively Attenuated Oligodendroglial Apoptosis Triggered by LPS Administration

In order to examine the influence of LPS infusion on the oligodendrocyte population in the hippocampus, dual immunolabelling for oligodendrocytes and active caspase-3 was performed. In controls, only 5 % oligodendroglia expressed caspase-3 (Figs. 3d, 5d). However, with LPS infusion there was a gradual increase in the number of colabelled cells in the hippocampus as compared to the controls (Figs. 3e, 5e). The morphometeric studies revealed that 44 % of the total oligodendroglial population at 14DPI co-expressed MAB1580 and active caspase-3 (Fig. 3B; $F_{(2,137)} = 9.775$; $P \leq 0.001$; Fig. 6) and most of these cells were in close proximity to CA3 region only (Fig. 3e). The number of apoptotic oligodendrocytes decreased from 21DPI onwards up to 42DPI with no significant difference from their respective controls (Fig. 3B).

Minocycline effectively restricted the oligodendroglial apoptosis as evident from our morphometric studies and only 9.6 % of the total oligodendroglia colabelled with caspase-3 at 14DPI (Figs. 3f, B, 5f; $F_{(2,137)} = 8.980$; $P \leq 0.001$; Fig. 6) in contrast to the 44 % in LPS-alone group animals. In all other parameters i.e. 21, 28 and 42DPI, the colabelled cells were very occasional.

Therapeutic Minocycline Administration Treatment Improves Neuronal Survival

Following LPS infusion only a slight difference in the number of caspase-3-labelled neurons was observed with respect to the vehicle controls (Figs. 4a, b) and the difference was only moderately significant at 14DPI (Fig. 4A, 6; $F_{(2,137)} = 3.827$; $P \leq 0.05$]. These 26 % colabelled cells were largely observed in the CA3 and DG regions only. However, a large number of non-colabelled caspase-3-positive cells in the entire hippocampal subfields pointed towards the apoptosis of non-neuronal cells.

Minocycline treatment to LPS-infused rats effectively inhibited the caspase-3-mediated neuronal apoptosis in the hippocampus at all-time points studied. Results showed only 10–12 % of active caspase-3-labelled neuronal cells throughout the hippocampus in minocycline-treated LPS-infused rats which was almost similar to the 10 % in controls (Fig. 6). Neuronal apoptosis evident at 14DPI following LPS infusion was significantly inhibited after minocycline treatment (Figs. 4c, A, 5i; $F_{(2,137)} = 4.533$; $P \leq 0.05$] and was maintained to the normal control values thereafter.

Minoycline Treatment Effectively Ameliorated Microglial Apoptosis in the LPS Exposed Animals

We next sought to determine whether LPS infusion caused microglial apoptosis by employing double immunolabelling with Iba1 and active caspase-3. To our surprise only 10 % of the total microglia colabelled with active caspase-3 quite similar to the controls (Fig. 4d, e), indicating that only a few microglial cells undergo LPS-induced caspase-3-mediated apoptosis as compared to 76 % astrocytes (Fig. 6). However, the total number of apoptotic microglia still remained significantly high at 7, 14 and 21DPI as compared to the controls (Fig. 4B; $F_{(2,137)} = 7.152, 4.563, 4.362$; $P \leq 0.01$ and $P \leq 0.05$). These colabelled microglia were found evenly scattered throughout the hippocampus. A gradual reduction in the number of colabelled cells was evaluated from 7DPI to 42DPI, and the values were restored near to the controls. Minocycline treatment to LPS-infused rats significantly reduced the caspase-3 + microglia population from 7-21 DPI, when peak number of colabelled cells were observed (Fig. 4f, B).

Discussion

In the present study we hypothesize that the LPS-induced inflammatory stimulus leads to an enhanced apoptosis of the activated astrocytes via caspase-3-mediated pathway. Minocycline treatment could effectively ameliorate the

LPS-induced inflammatory response in the hippocampus but could prevent astrocytic apoptosis only partially. Such selective astrocytic apoptosis could be primarily because of the glutamate-mediated excitotoxicity as evident from the increased expression of the EAAT2/GLT-1 transporter on the surface of the astrocytes following LPS infusion and downregulation of an astrocytic-specific enzyme, GS. Our study also confirms the earlier findings for the astrocytic and microglial activation and associated degeneration following LPS infusion (Castano et al. 1998; Saijo et al. 2009) and attenuatuation of apoptosis by minocycline treatment via inhibition of microglial activation in turn exerting its protective influence (Domercq and Matute 2004; Siq et al. 2004; Dutta and Basu 2011). Astrocytes being an important component of the tripartite synapse modulate neurotransmission and control extracellular level of neuroinflammation (Wegrzynowicz et al. 2011). The extracellular glutamate is efficiently uptaken through glutamate transporter EAAT2/GLT-1 (Tanaka et al. 1997), and is converted by GS into non-toxic glutamine which is then transported back to neurons (Choi et al. 1987; Shaked et al. 2002).

Growing evidences indicate that the inflammation and related excitotoxicity act as potential pathogenic factors in many central nervous system (CNS) diseases including neurodegenerative diseases and infections (Giovavnini et al. 2003; Zadori et al. 2012). Any stimulus leading to the glial activation would lead to the production of cytokines and inflammatory mediators that trigger neural damage (Blanco et al. 2005). The bacterial endototoxin, a major component of the Gram-negative bacterial cell wall has been extensively used as a glial activator for the induction of neuroinflammation and subsequent damage (Dutta et al. 2008; Burguillos et al. 2011; Patro et al. 2013). Astrocytes and microglia are regarded as immunocompetent cells of the innate immune system and respond to the LPS via Toll-like receptor-4 (TLR-4), producing inflammatory mediators ultimately leading to cellular apoptosis (Schubert and Ferroni 2003; Pickering et al. 2005; Lu et al. 2010). These findings thus support our results of increased microglial and astrocytic activation and consequent caspase-3-mediated apoptosis following LPS inflammation.

A significant reduction in the number of GS-positive astrocytes by 14DPI following LPS infusion in hippocampus is parallel to the increase in the number of apoptotic astrocytes evaluated which was also significant at 14DPI. In conditions of reduced GS expression the activated hypertrophied astrocytes fail to convert glutamate into glutamine leading to its retention and impaired glutamate homoeostatic system. Thus, increased GLT-1 and reduced GS expression seems to be major reasons for the apoptosis of activated astrocytes.

A unique mechanism of cellular injury in the CNS is excitotoxicity caused by excessive extracellular glutamate and the enhanced NMDA dependent signalling (al-Shabanah et al. 1996; McDonald et al. 1998; Wang and White 1999; Fern and Moller 2000; Domercq et al. 2007). Treatment of cultured mouse astrocytes with bacterial endotoxin LPS has been reported to cause an increased glutamate uptake as a result of altered expression and redistribution of EAATs/GLT-1 (Bowman et al. 2003; O'Shea et al. 2006; Liang et al. 2008; Tilleux and Hermans 2008). The elimination of activated astrocytes by apoptosis or the deactivation has been proposed to be a mechanism of autoregulation of activated astrocytes (Suk et al. 2001). Thus, the increase in GLT-1 expression on astrocytes in hippocampus following LPS (i.c.v) infusion indicates an increased glutamate uptake leading to their hypertrophy and activation. Such increased glutamate uptake in the conditions of reduced GS exerts its gliotoxic action on the hippocampal astrocytes leading to their apoptosis. These reports are in line with the earlier reports (Chen et al. 2000; Kim et al. 2010a, b; Paquet et al. 2013) indicating the astrocytic apoptosis via the oxidative stress-mediated apoptotic signalling pathway activated by gliotoxic action of glutamate. Olabarria et al. (2011) reported an age-dependent decrease in GS expression in the hippocampal astroglia of the triple-transgenic Alzheimer's disease mouse model and hypothesized that such astroglia fail to support neurons and control synapses due to the disease-associated pathological burden. Such changes in GS immunoreactivity indicate AD-related impairments of glutamate homoeostatic system, which may affect the efficacy of glutamatergic transmission contributing to cognitive deficiency. Thus, we propose GS as neuroprotective and its downregulation results in astroglial apoptosis as both the intracellular glutamate concentration and uptake of extracellular glutamate is dependent on glutamate metabolizing pathways.

Therapeutic minocycline treatment could not prevent the inflammation-associated astrocytic degeneration in LPS-treated rats. The results are in line with the studies stating that minocycline was ineffective in dampening the astrocytic activation (Tikka et al. 2001; Yoon et al. 2012; Haber et al. 2013). Matsukawa et al. (2009) were also reported that low-dose minocycline was protective to neurons in both in vivo and in vitro experimental models of stroke, while it provided no protection to astrocytes in the same models. These reports further support our finding that minocycline could not effectively combat both astrocytic activation and degeneration.

Microglia themselves are least susceptible to excitotoxicity because they express GluRs only when they are reactive, thus could be spared by glutamate-induced excitotoxicity following LPS infusion as occurs after ischaemia

(Gottlieb and Matute 1997) and in Alzheimer's disease (Kingham et al. 1999). However, an excessive and sustained activation of microglia is detrimental to neurons and oligodendrocytes both (Merrill et al. 1993; Bezzi et al. 2001; Polazzi and Contestabile 2002). Further the LPS-activated microglia are known to induce the death of oligodendroglia by releasing proinflammatory cytokines and chemokines and other intermediary molecules like reactive oxygen species and NO (Sherwin and Fern 2005; Li et al. 2005, 2008).

Oligodendrocytes are themselves vulnerable to excitotoxicity (Oka et al. 1993) and prolonged activation of GluRs is toxic to these cells in vitro and in vivo (Matute et al. 1997, 2006) thus explaining a sizeable number of oligodendroglial death occurring followed by LPS infusion. Domercq et al. (2007) also proposed that activated microglia compromise glutamate homoeostasis in cultured oligodendrocytes by blocking glutamate transporters leading to an increase in extracellular glutamate and subsequent death. In this study as well, the peak oligodendrocytic death recorded was at 14DPI preceding peak microglial activation at 7DPI in the LPS-infused animals, supporting thereby that the activated microglia release toxic molecules that in turn induce oligodendroglial excitotoxicity and death.

Minocycline reported to be a potent inhibitor of microglial activation (Kim and Suh 2009; Plane et al. 2010) and it inhibits LPS-induced microglial activation and subsequent cellular degeneration thereby exerting its neuroprotective influence by suppressing the associated inflammatory cascade (Domercq and Matute 2004; Siq et al. 2004; Dutta and Basu 2011). However, astrocytic activation and their subsequent apoptosis need further attention and therapeutic intervention.

In conclusion our data suggest that the efficient role of astrocytes in the prevention of glutamate-induced excitotoxic damage depends entirely on their ability to metabolically convert glutamate to glutamine by GS. In the conditions of increased GLT-1 and reduced GS expression following LPS exposure the activated hypertrophied astrocytes fail to effectively convert glutamate into glutamine, leading to its retention. This seems to be a major reason for the apoptosis of activated astrocytes via caspase-3-mediated pathway. In addition, this study also reveals that minocycline alone is not efficacious in reversing astrocytic degeneration caused by bacterial infection. Thus, future studies are required in which combinational therapy with glioprotectancts can be explored for their promising efficacy.

Acknowledgments We thankfully acknowledge the Department of Biotechnology, Ministry of Science and Technology, Govt. of India, New Delhi for providing the financial support. Facilities developed through the DBT-Human Resource Development and Bioinformatics Infrastructural Facility Programmes from Department of Biotechnology have also been used in this study.

Compliance with Ethical Standards

Conflict of interest The authors have no conflict of interest.

References

al-Shabanah OA, Mostafa YH, Hassan MT, Khairaldin AA, al-Sawaf HA (1996) Vitamin E protects against bacterial endotoxin-induced increase of plasma corticosterone and brain glutamate in the rat. Res Commun Mol Pathol Pharmacol 92(1):95–105

Bezzi P, Domercq M, Brambilla L, Galli R, Schols D, Clercq DE, Vescovi A, Bagetta G, Kollias G, Meldolesi J, Volterra A (2001) CXCR4-activated astrocyte glutamate release via TNF-α: amplification by microglia triggers neurotoxicity. Nat Neurosci 4(7):702–710

Blanc EM, Bruce-Keller AJ, Mattson MP (1998) Astrocytic gap junctional communication decreases neuronal vulnerability to oxidative stress-induced disruption of Ca2+ homeostasis and cell death. J Neurochem 70(3):958–970

Blanco AM, Valles SL, Pascual M, Guerri C (2005) Involvement of TLR4/type I IL-1 receptor signalling in the induction of inflammatory mediators and cell death induced by ethanol in cultured astrocytes. J Immunol 175:6893–6899

Bowman CC, Rasley A, Tranguch SL, Marriott I (2003) Cultured astrocytes express toll-like receptors for bacterial products. Glia 43:281–291

Burguillos MA, Deierborg T, Kavanagh E, Persson A, Hajji N, Garcia-Quintanilla A, Cano J, Brundin P, Englund E, Venero JL, Joseph B (2011) Caspase signalling controls microglia activation and neurotoxicity. Nature 472(7343):319–324

Cai ZY, Yan Y, Chen R (2010) Minocycline reduces astrocytic reactivation and neuroinflammation in the hippocampus of a vascular cognitive impairment rat model. Neurosci Bull 26(1):28–36

Caruso C, Durand D, Schioth HB, Rey R, Seilicovich A, Lasaga M (2007) Activation of melanocortin 4 receptors reduces the inflammatory response and prevents apoptosis induced by lipopolysaccharide and interferon-γ in astrocytes. Endocrinology 148:4918–4926

Castano A, Herrara AJ, Cano J, Machado A (1998) Lipopolysaccharide intranigral injection induces inflammatory reaction and damage in nigrostriatal dopaminergic system. J Neurochem 70:1584–1592

Chen Y, Swanson RA (2003) Astrocytes and brain injury. J Cereb Blood Flow Metab 23:137–149

Chen CJ, Liao SL, Kuo JS (2000) Gliotoxic action of glutamate on cultured astrocytes. J Neurochem 75:1557–1565

Choi DW, Maulucci Gedde MA, Kriegstein AR (1987) Glutamate neurotoxicity in cortical cell culture. J Neurosci 7:357–368

Claycomb KI, Johnson KM, Winokur PN, Sacino AV, Crocker SJ (2013) Astrocyte regulation of CNS inflammation and remyelination. Brain Sci 3:1109–1127

Danbolt NC (2001) Glutamate uptake. Progr Neurobiol 65:1–105

Domercq M, Matute C (2004) Neuroprotection by tetracyclines. Trends Pharmacol Sci 25(12):609–612

Domercq M, Sanchez-Gomez MV, Sherwin C, Etxebarria E, Fern R, Matute C (2007) System xc^- and glutamate transporter inhibition mediates microglial toxicity to oligodendrocytes. J Immunol 178:6549–6556

Dutta K, Basu A (2011) Use of minocycline in viral infections. Indian J Med Res 133:467–470

Dutta G, Zhang P, Liu B (2008) The lipopolysaccharide Parkinson's disease animal model: mechanistic studies and drug discovery. Fundam Clin Pharmacol 22(5):453–464

Endale M, Kim SD, Lee WM, Kim S, Suk K, Cho JY, Park HJ, Wagley Y, Kim S, Oh JW, Rhee MH (2010) Ischemia induces regulator of G protein signaling 2 (RGS2) protein upregulation and enhances apoptosis in astrocytes. Am J Physiol Cell Physiol 298(3):C611–C623

Felts PA, Woolston AM, Fernando HB, Asquith S, Gregson NA, Mizzi OJ, Smith KJ (2005) Inflammation and primary demyelination induced by the intraspinal injection of lipopolysaccharide. Brain 128:1649–1666

Fern R, Moller T (2000) Rapid ischemic cell death in immature oligodendrocytes: a fatal glutamate release feedback loop. J Neurosci 20:34–42

Garcia-Segura LM, Mccarthy MM (2004) Minireview: role of glia in neuroendocrine function. Endocrinology 145:1082–1086

Ghosh A, Birngruber T, Sattler W, Kroath T, Ratzer M, Sinner F, Pieber TR (2014) Assessment of blood brain barrier function and the neuroinflammatory response in the rat brain by using cerebral open flow microperfusion (cOFM). PLoS ONE 9(5):e98143

Giovavnini MG, Scali C, Prosperi C, Bellucci A, Pepeu G, Casamenti F (2003) Experimental brain inflammation and neurodegeneration as model of Alzheimer's disease: protective effects of selective COX-2 inhibitors. Int J Immunopathol Pharmacol 16:31–40

Gottlieb M, Matute C (1997) Expression of ionotropic glutamate receptor subunits in glial cells of the hippocampal CA1 area following transient forebrain ischemia. J Cereb Blood Flow Metab 17:290–300

Guimaraes JS, Freire MA, Lima RR, Picanço-Diniz CW, Pereira A, Gomes-Leal W (2010) Minocycline treatment reduces white matter damage after excitotoxic striatal injury. Brain Res 1329:182–193

Haber M, Abdel Baki SG, Grin'kina MN, Irizarry R, Ershova A, Orsi S, Grill RJ, Dash P, Bergold PJ (2013) Minocycline plus N-acetylcysteine synergize to modulate inflammation and prevent cognitive and memory deficits in a rat model of mild traumatic brain injury. Exp Neurol 249:169–177

Haydon PG, Carmignoto G (2006) Astrocyte control of synaptic transmission and neurovascular coupling. Physiol Rev 86:1009–1031

Henry CJ, Huang Y, Wynne A, Hanke M, Himler J, Bailey MT, Sheridan JF, Godbout JP (2008) Minocycline attenuates lipopolysaccharide (LPS) induced neuroinflammation, sickness behaviour and anhedonia. J Neuroinflammation 5:15

Huang TL, O'Banion MK (1998) Interleukin-1 beta and tumor necrosis factor-alpha suppress dexamethasone induction of glutamine synthetase in primary mouse astrocytes. J Neurochem 71:1436–1442

Kim HS, Suh YH (2009) Minocycline and neurodegenerative diseases. Behav Brain Res 196(2):168–179

Kim JH, Min KJ, Seol W, Jou I, Joe EH (2010a) Astrocytes in injury states rapidly produce anti-inflammatory factors and attenuate microglial inflammatory responses. J Neurochem 115(5):1161–1171

Kim SH, Han YJ, Park JH, Yoo SJ (2010b) Glutamate induces endoplasmic reticulum stress-mediated apoptosis in primary rat astrocytes. J Korean Geriatr Soc 14(4):242–252

Kingham PJ, Cuzner ML, Pocock JM (1999) Apoptotic pathways mobilized in microglia and neurons as a consequence of chromogranin-A induced microglial activation. J Neurochem 73:538–547

Kirchhoff F, Dringen R, Giaume C (2001) Pathways of neuron-astrocyte interactions and their possible role in neuroprotection. Eur Arch Psychiatry Clin Neurosci 251(4):159–169

Kreutzberg GW (1996) Microglia: a sensor for pathological events in the CNS. Trends Neurosci 19:312–318

Leonardo CC, Eakin AK, Ajmo JM, Collier LA, Pennypacker KR, Strongin AY, Gottschall PE (2008) Delayed administration of a matrix metalloproteinase inhibitor limits progressive brain injury after hypoxia–ischemia in the neonatal rat. J Neuroinflammation 5:34

Li J, Baud O, Vartanian T, Volpe JJ, Rosenberg PA (2005) Peroxynitrite generated by inducible nitric oxide synthase and NADPH oxidase mediates microglial toxicity to oligodendrocytes. Proc Natl Acad Sci USA 102:9936–9941

Li J, Ramenaden ER, Peng J, Koito H, Volpe JJ, Rosenberg PA (2008) Tumor necrosis factor alpha mediates lipopolysaccharide-induced microglial toxicity to developing oligodendrocytes when astrocytes are present. J Neurosci 28(20):5321–5330

Liang J, Takeuchi H, Doi Y, Kawanokuchi J, Sonobe Y, Jin S, Yawata I, Li H, Yasuoka S, Mizuno T, Suzumura A (2008) Excitatory amino acid transporter expression by astrocytes is neuroprotective against microglial excitotoxicity. Brain Res 1210:11–19

Lu DY, Tang CH, Chen YH, Wei IH (2010) Berberine suppresses neuroinflammatory responses through AMP-activated protein kinase activation in BV-2 microglia. J Cell Biochem 110:697–705

Maragakis NJ, Rothstein JD (2004) Glutamate transporters: animal models to neurologic disease. Neurobiol Dis 15:461–473

Matsukawa N, Yasuhara T, Hara K, Xu L, Maki M, Yu G, Kaneko Y, OjikaK HessDC, Borlongan CV (2009) Therapeutic targets and limits of minocycline neuroprotection in experimental ischemic stroke. BMC Neurosci 10:126

Matute C, Sanchez-Gomez MV, Martinez-Millan L, Miledi R (1997) Glutamate receptor-mediated toxicity in optic nerve oligodendrocytes. Proc Natl Acad Sci USA 94:8830–8835

Matute C, Domercq M, Sanchez-Gomez MV (2006) Glutamate-mediated glial injury: mechanisms and clinical importance. Glia 53:212–224

McDonald JW, Althomsons SP, Hyrc KL, Choi DW, Goldberg MP (1998) Oligodendrocytes from forebrain are highly vulnerable to AMPA/kainate receptor-mediated excitotoxicity. Nat Med 4:291–297

Merrill JE, Ignarro LJ, Sherman MP, Melinek J, Lane TE (1993) Microglial cell cytotoxicity of oligodendrocytes is mediated through nitric oxide. J Immunol 151:2132–2141

Oka A, Belliveau MJ, Rosenberg PA, Volpe JJ (1993) Vulnerability of oligodendroglia to glutamate: pharmacology, mechanisms, and prevention. J Neurosci 13:1441–1453

Olabarria M, Noristani HN, Verkhratskyand A, Rodríguez JJ (2011) Age-dependent decrease in glutamine synthetase expression in the hippocampal astroglia of the triple transgenic Alzheimer's disease mouse model: mechanism for deficient glutamatergic transmission? Mol Neurodegener 6:55

Oliver CN, Starke-Reed PE, Stadtman ER, Liu GJ, Carney JM, Floyd RA (1990) Oxidative damage to brain proteins, loss of glutamine synthetase activity, and production of free radicals during ischemia/reperfusion-induced injury to gerbil brain. Proc Natl Acad Sci USA 87:5144–5147

O'Shea RD, Lau CL, Farso MC, Diwakarla S, Zagami CJ, Svendsen BB, Feeney SJ, Callaway JK, Jones NM, Pow DV, Danbolt NC, Jarrott B, Beart PM (2006) Effects of lipopolysaccharide on glial phenotype and activity of glutamate transporters: evidence for delayed up-regulation and redistribution of GLT-1. Neurochem Int 48:604–610

Paquet M, Ribeiro FM, Guadagno J, Jessica L, Esseltine JL, Ferguson SSG, Cregan SP (2013) Role of metabotropic glutamate receptor 5 signaling and homer in oxygen glucose deprivation-mediated astrocyte apoptosis. Mol Brain 6:9

Patro N, Singh K, Patro I (2013) Differential microglial and astrocytic response to bacterial and viral infection in the developing hippocampus of neonatal rats. IJEB 51:606–614

Paxinos G, Watson C (1982) The rat brain in stereotaxic coordinates. Academic Press, San Diego

Pickering M, Cumiskey D, O'Connor JJ (2005) Actions of TNF-alpha on glutamatergic synaptic transmission in the central nervous system. Exp Physiol 90:663–670

Plane JM, Shen Y, Pleasure DE, Deng W (2010) Prospects for minocycline neuroprotection. Arch Neurol 67(12):1442–1448

Polazzi E, Contestabile A (2002) Reciprocal interactions between microglia and neurons: from survival to neuropathology. Rev Neurosci 13:221–242

Quintas C, Pinho D, Pereira C, Saraiva L, Goncalves J, Queiroz G (2014) Microglia P2Y6 receptors mediate nitric oxiderelease and astrocyte apoptosis. J Neuroinflammation 11:141–152

Saijo K, Winner B, Carson CT, Collier JG, Boyer L, Rosenfeld MG, Gage FH, Glass CK (2009) A Nurr1/CoREST pathway in microglia and astrocytes protects dopaminergic neurons from inflammation induced death. Cell 137:47–59

Schousboe A, Belhage B, Frandsen A (1997) Role of Ca+2 and other second messengers in excitatory amino acid receptor mediated neurodegeneration: clinical perspectives. Clin Neurosci 4(4):194–198

Schubert P, Ferroni S (2003) Pathological glial reactions in neurodegenerative disorders: prospects for future therapeutics. Expert Rev Neurother 3(3):279–287

Shaked I, Ben-Dror I, Vardimon L (2002) Glutamine synthetase enhances the clearance of extracellular glutamate by the neural retina. J Neurochem 83:574–580

Sherwin C, Fern R (2005) Acute lipopolysaccharide-mediated injury in neonatal white matter glia: role of TNF-α, IL-1β, and calcium. J Immunol 175:155–161

Si Q, Cosenza MA, Kim MO, Zhao ML, Brownlee M, Goldstein H, Lee SC (2004) A novel action of minocycline: inhibition of human immunodeficiency virus type 1 infection in microglia. J Neurovirol 10(5):284–292

Sofroniew MV, Vinters HV (2010) Astrocytes: biology and pathology. Acta Neuropathol 119:7–35

Suk K, Lee J, Hur J, Kim YS, Lee M, Cha S, Kim S, Kim H (2001) Activation-induced cell death of rat astrocytes. Brain Res 900:342–347

Takuma K, Baba A, Matsuda T (2004) Astrocyte apoptosis: implications for neuroprotection. Prog Neurobiol 72:111–127

Tanaka K, Watase K, Manabe T, Yamada K, Watanabe M, Takahashi K, Iwama H, Nishikawa T, Ichihara N, Kikuchi T, Okuyama S, Kawashima N, Hori S, Takimoto M, Wada K (1997) Epilepsy and exacerbation of brain injury in mice lacking the glutamate transporter GLT-1. Science 276:1699–1702

Tikka T, Fiebich BL, Goldsteins G, Keinanen R, Koistinaho J (2001) Minocycline, a tetracycline derivative, is neuroprotective against excitotoxicity by inhibiting activation and proliferation of microglia. J Neurosci 21(8):2580–2588

Tilleux S, Hermans E (2008) Down-regulation of astrocytic GLAST by microglia-related inflammation is abrogated in dibutyryl camp-differentiated cultures. J Neurochem 105(6):2224–2236

Tilleux S, Berger J, Hermans E (2007) Induction of astrogliosis by activated microglia is associated with a down-regulation of metabotropic glutamate receptor 5. J Neuroimmunol 189(1–2):23–30

Verkhratsky A, Butt A (2007) Glial neurobiology. A textbook. Wiley, Chichester

Wang YS, White TD (1999) The bacterial endotoxin lipopolysaccharide causes rapid inappropriate excitation in rat cortex. J Neurochem 72:652–660

Wegrzynowicz MS, Wegrzynowicz M, Lee E, Bowman AB, Aschner M (2011) Role of astrocytes in brain function and disease. Toxicol Pathol 39(1):115–123

Yoon SY, Patel D, Dougherty PM (2012) Minocycline blocks lipopolysaccharide induced hyperalgesia by suppression of microglia but not astrocytes. Neuroscience 221:214–224

Yrjanheikki J, Keinanen R, Pellikka M, Hokfelt T, Koistinaho J (1998) Tetracyclines inhibit microglial activation and are neuroprotective in global brain ischemia. Proc Natl Acad Sci USA 95:15769–15774

Zadori D, Klivenyi P, Szalardy L, Fulop F, Toldi J, Vecsei L (2012) Mitochondrial disturbances, excitotoxicity, neuroinflammation and kynurenines: novel therapeutic strategies for neurodegenerative disorders. J Neurol Sci 322:187–191

Zhao G, Flavin MP (2000) Differential sensitivity of rat hippocampal and cortical astrocytes to oxygen-glucose deprivation injury. Neurosci Lett 285:177–180